



Enabling drug discovery for the PARP protein family through the detection of mono-ADP-ribosylation

Alvin Z. Lu^a, Ryan Abo^a, Yue Ren^b, Bin Gui^a, Jan-Rung Mo^a, Danielle Blackwell^b, Tim Wigle^b, Heike Keilhack^a, Mario Niepel^{a,*}

^a Department of Biological Sciences, Ribon Therapeutics, Inc., Cambridge, MA 02140, United States

^b Department of Molecular Discovery, Ribon Therapeutics, Inc., Cambridge, MA 02140, United States

ARTICLE INFO

Keywords:

PARP
Mono-ADP-ribosylation
Substrate identification
MARylation assay
PARP inhibitors
Detection reagents

ABSTRACT

Poly-ADP-ribose polymerases (PARPs) are a family of enzymes responsible for transferring individual or chains of ADP-ribose subunits to substrate targets as a type of post-translational modification. PARPs regulate a wide variety of important cellular processes, ranging from DNA damage repair to antiviral response. However, most research to date has focused primarily on the polyPARPs, which catalyze the formation of ADP-ribose polymer chains, while the monoPARPs, which transfer individual ADP-ribose monomers, have not been studied as thoroughly. This is partially due to the lack of robust assays to measure mono-ADP-ribosylation in the cell. In this study, the recently developed MAR/PAR antibody has been shown to detect mono-ADP-ribosylation in cells, enabling the field to investigate the function and therapeutic potential of monoPARPs. In this study, the antibody was used in conjunction with engineered cell lines that overexpress various PARPs to establish a panel of assays to evaluate the potencies of literature-reported PARP inhibitors. These assays should be generally applicable to other PARP family members for future compound screening efforts. A convenient and generalizable workflow to identify and validate PARP substrates has been established. As an initial demonstration, aryl hydrocarbon receptor was verified as a direct PARP7 substrate and other novel substrates for this enzyme were also identified and validated. This workflow takes advantage of commercially available detection reagents and conventional mass spectrometry instrumentation and methods. Ultimately, these assays and methods will help drive research in the PARP field and benefit future therapeutics development.

1. Introduction

Poly-ADP-ribose polymerases (PARPs) catalyze the transfer of the ADP-ribose moiety of NAD⁺ to various targets, releasing nicotinamide in the process [1–4]. There are 17 PARPs in humans, all of which contain a common catalytic domain of ~230 amino acids [2]. Despite their name, only four of these enzymes (PARP1, 2, 5a, and 5b) actually catalyze the synthesis of a poly-ADP-ribose (PAR) chain attached to their target substrates [4]. The rest of the family members are termed monoPARPs, which only transfer a single mono-ADP-ribose (MAR) moiety, with the exception of PARP13, which appears to lack ADP-ribose transferase activity [1,5].

PARPs are involved in a wide variety of cellular processes [6]. Most notably, PARP1 synthesizes poly-ADP-ribose chains in the nucleus that serve as a scaffold for DNA repair for the recruitment of DNA repair proteins containing PAR-binding modules to sites of DNA damage [3]. ADP-ribosylation has also been described in numerous other cellular

processes, including protein degradation, stress response, RNA processing, mitotic spindle formation, chromatin decondensation, retroviral silencing, cell metabolism, and cell-cycle regulation [6,7].

Despite the importance of this enzyme family, the study of this post-translational modification that they produce has been limited due to a lack of robust and convenient detection reagents. The development of a PAR-binding antibody in the 1980s has enabled researchers to elucidate the role of PARP1 in DNA damage repair over the ensuing decades [8–12]. However, the development of tools and reagents to study MARylation has lagged behind. In contrast to protein phosphorylation, where the development of phospho-specific antibodies has empowered thorough investigation of a wide variety of kinase family members, no site-specific MAR antibodies have been available that can achieve detection of this post-translational modification in common cell biology techniques such as Western blotting or immunofluorescence. As an alternative, the PARP field has relied upon ADP-ribose-binding domains found in natural proteins to detect this modification [13,14]. These

* Corresponding author.

E-mail address: mniepel@ribontx.com (M. Niepel).

<https://doi.org/10.1016/j.bcp.2019.05.007>

Received 28 March 2019; Accepted 6 May 2019

Available online 07 May 2019

0006-2952/ © 2019 The Authors. Published by Elsevier Inc. This is an open access article under the CC BY-NC-ND license

(<http://creativecommons.org/licenses/by-nc-nd/4.0/>).

“reader” domains include the PAR-binding zinc-finger (PBZ) domain that recognizes adjacent ADP-ribose groups of PAR chain, the WWE domains that bind iso-ADP-ribose, and the macrodomain module that binds to terminal ADP-ribose [1]. Recently, antibody-like binding reagents based on these domains have been developed and commercialized for the study of PARP biology [5,15].

To elucidate the biological pathways in which PARPs participate, it is important to identify their substrates. The macrodomain of Af1521 from the archaeobacteria *Archaeoglobus fulgidus* was first used by Dani and colleagues as an affinity purification method, and subsequently coupled to mass spectrometry to identify ADP-ribosylated substrates from the cell [13]. Since then, others have used similar strategies to enrich for PARylated proteins after subjecting cells to DNA damaging treatments that activate PARP1 [11,14]. Poly-ADP-ribose glycohydrolase (PARG) contains a macrodomain-like structure, and a catalytically dead version of PARG was used for affinity enrichment to complement Af1521 and the PAR-binding antibody 10H [11]. Alternatively, boronate affinity has been used to isolate and quantitate ADP-ribose through chemical coupling with the *cis*-diol group of the ribose [16,17]. This strategy was combined with hydroxylamine elution to successfully define ADP-ribosylated glutamate and aspartate residues in the human proteome [18]. More recently, a chemical genetics approach has shown the potential of combining a clickable NAD⁺ analogue and the engineering of analogue-sensitive PARPs in identifying their substrates [19]. In this so-called “bump-and-hole approach”, the engineered PARPs transfer the ADPr moiety carrying a clickable group to substrate proteins as a handle for enrichment and subsequent identification [20–22]. However, one drawback of this approach is that it requires significant effort to find the most suitable pair of PARP mutant and NAD⁺ analogue, thereby making it challenging to generalize across different PARPs. In addition, NAD⁺ analogs are often not cell permeable preventing the identification of substrates from intact cell systems. Other, more general approaches such as proximity-dependent labeling and protein arrays have also aided in the discovery of PARP substrates [22,23]. Moreover, growing interest in PARP-specific inhibitors has led to the continuous development of new tool compounds to identify and validate PARP substrates [6,24].

Compared to the well-studied PARP1, there are limited number of reports on substrates of PARPs that perform MARYlation. PARP16 has been shown to ADP-ribosylate itself, PERK, and IRE1 α in response to endoplasmic reticulum stress by regulating the unfolded protein response (UPR) [25]. PARP10 has recently been reported to suppress tumor metastasis by MARYlating Aurora A and thereby inhibiting its kinase activity [26,27]. PARP6 inhibition and knockdown have been shown to correlate with induction of multipolar spindle formation, a phenotype that was attributed to direct modification of Chk1 [23]. PARP14 has been found to MARYlate the catalytically inactive PARP13, which has a known role in regulating RNA stability [22]. PARP7, or the TCDD-inducible PARP (TIPARP), has been reported to play a role in stress response via MARYlation of the aryl hydrocarbon receptor (AHR), which regulates many gene expression pathways including those involved with xenobiotic metabolism and cell cycle control [28,29]. In general, however, the field has been challenged by the lack of convenient biochemical methods to identify and validate monoPARP substrates.

In this study, the performance of commercially-available affinity reagents were compared, including a pan-ADP-ribose binding reagent, a mono-ADP-ribose binding reagent, and a MAR/PAR antibody. Cell lines were engineered that stably overexpress various PARPs, and confirmed the increased PARP-specific ADP-ribosylation on Western blots as measured by the MAR/PAR antibody. This system was used to establish biochemical assays based on immunofluorescence staining of these cell lines, demonstrating a viable approach for assessing the effects of treatments in a cellular context. Next, a PARP7 overexpressing cell line was employed as a reporter system to show that MG132, a proteasome inhibitor, can induce cytoplasmic accumulation of PARP7 and modulate

its MARYlation activity. Lastly, a general workflow was established to identify monoPARP substrates and validate their MARYlation by PARP7. These easily accessible tools and methods will benefit ongoing efforts to investigate PARP function in drug discovery and basic research.

2. Materials and methods

2.1. Chemicals, antibodies, and proteins

Antibodies for DDX5, RBM14, and hnRNP H were obtained from Abcam (Cambridge, UK). Olaparib [30,31] and PJ34 hydrochloride [32] were obtained from AdooQ Bioscience (Irvine, CA). Histone H3 and talazoparib [33] were obtained from BPS Bioscience (San Diego, CA). MAR/PAR, β -actin, and AHR antibodies were obtained from Cell Signaling Technology (Danvers, MA). Anti-SBP-tag antibody, anti-pan-ADP-ribose binding reagent, and anti-mono-ADP-ribose binding reagent were obtained from EMD Millipore (Burlington, MA). Veliparib [34], ME0327 [35], ME0328 [35,36], XAV-939 [37], and OUL35 [38] were obtained from Pharmaron (Beijing, China). Poly-ADP-ribose antibody (10H) was obtained from Santa Cruz Biotechnology (Santa Cruz, CA). Rucaparib [39], niraparib [40], NMS-P118 [41], and UPF1069 [42] were obtained from Selleckchem (Houston, TX). AZ12629495 (patent WO 2016/116602) and PARG inhibitor were obtained from SYNthesis (Suzhou, China). Bovine serum albumin (BSA) and blue carrier (BC) were obtained from Thermo Fisher Scientific (Waltham, MA). Af1521 resin was obtained from Tulip Biolabs (Lansdale, PA). Protein preps of PARP1, PARP3, catalytic domain of PARP10 (aa 808–1025) were produced at Viva Biotech (Shanghai, China). A monoclonal PARP7 antibody was generated against “specify antigen” at Genscript (Nanjing, China). PARP16 antibody and cholera toxin A protein were obtained from Sigma-Aldrich (St Louis, MO). ADPr, NAD⁺, ATP, AMP, FAD, adenosine, thymine, cytidine, guanine, doxycycline, and MG132 were obtained from Sigma-Aldrich (St Louis, MO).

2.2. Peptides, DNA oligos, and cell lines

The PARP10-derived peptide (sequence: CRRPVEQVLYH) was generated at Biopeptide Co. (San Diego, CA). Duplex DNA (sequence: 5'-ACCCGTGCTGTGGGC/ideoxyU/GGAGAACAAGGTGAT-3'), dumbbell DNA (sequence: 5'-phos-GCTGGCTTCGTAAGAAGCCAGCTCGCGGTCA GCTTGCTGACCGCG-3') were ordered from Integrated DNA Technologies (Coralville, Iowa). SK-MES-1, A549, HeLa, HARA, and EBC-1 cell lines were obtained from ATCC (Manassas, VA).

2.3. Biochemical ADP-ribosylation of recombinant proteins and dot blotting

All ADP-ribosylation reactions were carried out in buffer containing 50 mM HEPES pH 7.2, 150 mM NaCl, and 2 mM TCEP. After incubation, reactions were stopped by dilution in 6 M guanidine hydrochloride. Five μ M full-length PARP1 was incubated with 600 μ M NAD⁺ and 1 μ M duplex DNA for 10 min at room temperature. Ten μ M full-length PARP3 was incubated with 600 μ M NAD⁺ and 1 μ M dumbbell DNA overnight at room temperature. Cholera toxin A at 0.2 mg/mL was incubated with 400 μ M NAD⁺ at 30 °C overnight. One μ M of peptide comprising the PARP10 catalytic domain was incubated with 20 μ M histone H3 and 600 μ M NAD⁺ at room temperature overnight. The short peptide derived from PARP10 (sequence: CRRPVEQVLYH) was first conjugated to either BSA or BC by maleimide chemistry according to the manufacturer's protocol. Twenty μ M BSA-peptide or BC-peptide was then incubated with 1 μ M PARP10 catalytic domain and 600 μ M NAD⁺ at room temperature overnight. The PARP10 protein with an N-terminal 6xHis tag was cleared from the histone H3, BSA-peptide, and BC-peptide preps using Dynabeads His-Tag purification resin (Thermo Fisher Scientific, Waltham, MA).

Modified and unmodified proteins were diluted to 50, 25, 10, or

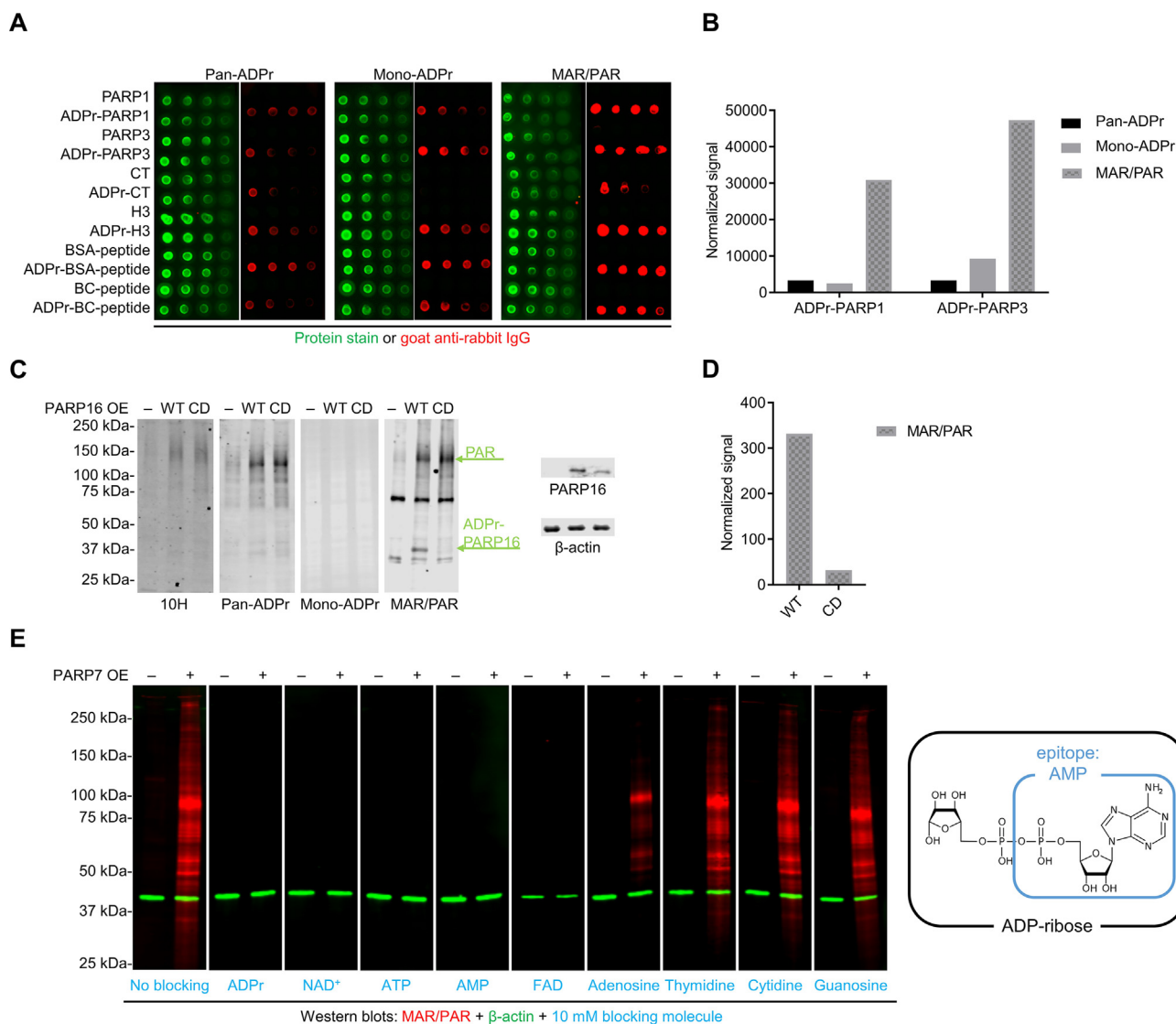


Fig. 1. Validation and characterization of the MAR/PAR antibody. A) Binding reagents were tested by dot blot against a panel of unmodified and modified proteins. 50, 25, 10, and 5 ng of each samples were spotted from left to right on nitrocellulose membranes, stained with the REVERT protein stain, and then incubated with the indicated primary affinity reagents followed by detection using goat anti-rabbit IgG secondary antibody. CT: cholera toxin; H3: histone H3; BC: Blue Carrier. B) Secondary antibody signals were quantified and normalized against protein stain for ADP-ribosylated PARP1 and PARP3. C) Western blots of lysates from HeLa PARP16 knockout cells transiently transfected with either wild-type (WT) or catalytically dead (CD) PARP16. Primary staining was performed with the three ADP-ribosylation affinity reagents as well as the 10H PAR-binding antibody. D) MAR/PAR signals of PARP16 were quantified and normalized against overexpression levels as detected by PARP16 antibody. E) Western blot with MAR/PAR antibody against SK-MES-1 cells that stably overexpress SBP-tagged PARP7. Cells were treated with DMSO or 1 μ g/mL doxycycline for 24 h to induce PARP7 overexpression. Blots were incubated with MAR/PAR antibody in absence or presence of different blocking molecules, listed at the bottom of each panel.

5 ng/ μ L in 6 M guanidine hydrochloride. 1 μ L of each sample was spotted on nitrocellulose membrane (BioRad, Hercules, CA), which was air dried for 15 min and rinsed once in water. The membrane was stained with REVERT protein stain (LI-COR, Lincoln, NE) according to manufacturer's recommended protocol and scanned on the Odyssey CLx infrared imaging system. The membrane was blocked for 2 h at room temperature in TBS Odyssey Blocking Buffer (LI-COR, Lincoln, NE), followed by incubation with primary affinity reagent. The membrane was washed with TBS-T and then incubated with 800 IRDye-conjugated goat anti-rabbit secondary antibodies (LI-COR, Lincoln, NE) for 1 h at room temperature. After washing with TBS-T, the blot was scanned on the Odyssey CLx infrared imaging system.

2.4. Transient expression of PARP16

Wild-type and catalytically dead (H152Q, Y182A) PARP16 overexpression plasmids were generated at Viva Biotech (Shanghai, China). HeLa PARP16 CRISPR knockout cell line (single cell clone) was generated at ChemPartner (Shanghai, China) using guide RNAs with the sequences AAAGTCCTTACAGTCGCCGGGG and CCGACAAGTGCCTCTGCCGGGG. Cells were seeded in Corning 6-well plates (Corning, NY) and grown to 80% confluence. Plasmids were mixed with Lipofectamine 3000 in Opti-MEM (Thermo Fisher Scientific, Waltham, MA) according to the manufacturer's recommended protocol. The DNA-lipid mixture was incubated with the cells for 8 h at 37 $^{\circ}$ C, after which the media was replaced with DMEM (Thermo Fisher Scientific, Waltham, MA) supplemented with 10% FBS (VWR, Radnor, PA). The cells were then incubated overnight at 37 $^{\circ}$ C.

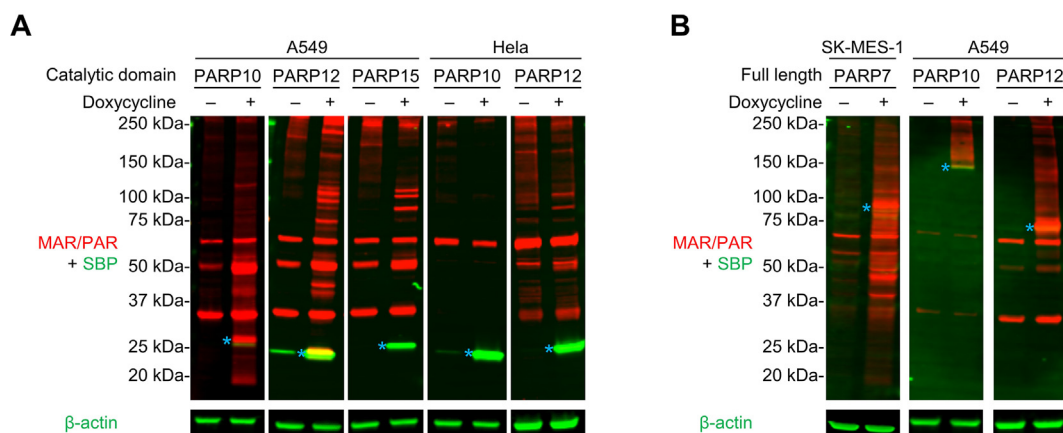


Fig. 2. MAR/PAR antibody detects ADP-ribosylation banding patterns associated with overexpression of monoPARPs in A) A549 or HeLa cells stably overexpressing the catalytic domain of PARP10 (residues 808–1025), PARP12 (residues 489–684), or PARP15 (residues 481–678) and B) SK-MES-1 or A549 cells stably overexpressing full-length PARP7, 10, or 12. Expression was induced with 1 $\mu\text{g}/\text{mL}$ doxycycline for 24 h. Blue asterisks indicate bands representing the overexpressed monoPARPs as detected by anti-SBP antibody.

2.5. Generation of stable PARP overexpression cell lines

Full length or catalytic domain sequences of various PARPs with an N-terminal SBP tag were subcloned at Viva Biotech (Shanghai, China) into the pInducer10 vector (Addgene, Watertown, MA) carrying the tetracycline-response element and puromycin resistance gene. These were then packaged into lentivirus and purified at Vigene Biosciences (Rockville, MD). Parental cell lines (SK-MES-1, A549, or HeLa) were transduced at a multiplicity of infection (MOI) of 10 in the presence of 8 $\mu\text{g}/\text{mL}$ polybrene (Thermo Fisher Scientific, Waltham, MA) for 2 days. Modified cells were selected with 1 $\mu\text{g}/\text{mL}$ of puromycin for at least a week with appropriate media changes. Surviving cells were grown, maintained, and split in media with 1 $\mu\text{g}/\text{mL}$ of puromycin (Thermo Fisher Scientific, Waltham, MA). Expression of the transgenes was induced with 1 $\mu\text{g}/\text{mL}$ of doxycycline in growth media for 24 h.

2.6. Cell lysis and Western blotting

Freshly cultured cells post doxycycline treatment were washed with PBS and lysed directly on plate in M-PER buffer (Thermo Fisher Scientific, Waltham, MA) supplemented with 10 μM PARG inhibitor, 1 μM AZ12629495, 1 μM TCEP, and 1X Halt protease, and phosphatase inhibitor cocktail (Thermo Fisher Scientific, Waltham, MA). Cell lysate was cleared by centrifugation at 15,000 $\times g$ for 10 min. Cleared samples were prepared in 4X protein sample loading buffer (LI-COR, Lincoln, NE) and heated to 65 $^{\circ}\text{C}$ for 5 min, and then run on 4–20% TGX polyacrylamide gels (Bio-Rad, Hercules, CA). Proteins in the gel were transferred to a piece of Immobilon-FL PVDF membrane (EMD Millipore, Burlington, MA) using the TransBlot Turbo (BioRad, Hercules, CA) semi-dry transfer setup. The membrane was blocked in TBS Odyssey Blocking Buffer (LI-COR, Lincoln, NE) for at least 2 h, followed by incubation with primary antibodies for 2 h at room temperature. The membrane was washed with TBS-T and then incubated with 680 or 800 IRDye-conjugated donkey anti-mouse and/or goat anti-rabbit secondary antibodies (LI-COR, Lincoln, NE) for 1 h at room temperature. After washing with TBS-T, the blot was scanned on the Odyssey CLx infrared imaging system.

2.7. Immunofluorescence

Cells were seeded on a 384-well or 96-well Corning clear bottom black plate at a density of 3500 cells/well or 10,000 cells/well, respectively, and allowed to attach overnight. For the PARP7, PARP10, PARP12, PARP15 assays, cells were treated with 1 $\mu\text{g}/\text{mL}$ of

doxycycline to induce PARP overexpression and incubated with various PARP inhibitors for 24 h. For the PARP1 assay, cells were incubated with inhibitors for 24 h and then stimulated with hydrogen peroxide for 10 min prior to fixation. For methanol fixation, the media was removed from the plate before adding 100% ice-cold methanol and incubating for 30 min at -20°C . For paraformaldehyde (PFA) fixation, one part 12% PFA was added to two parts culture media for a 4% working concentration, and cells were incubated in this PFA mixture at room temperature for 30 min. After fixation, the cells were washed with PBS and permeabilized with 0.5% Triton X-100 in PBS for 30 min. The plate was blocked with Odyssey Blocking Buffer for 2 h at room temperature and incubated with primary antibodies overnight at 4 $^{\circ}\text{C}$. MAR/PAR antibody and SBP antibody were used at 1:1000 dilution in TBS Odyssey Blocking Buffer (LI-COR) for immunofluorescence. The plate was washed three times with PBS-T followed by incubation with Alexa488-conjugated anti-mouse and Alexa647-conjugated anti-rabbit secondary antibodies at 1:1000 dilution and 4 μM Hoechst 33342 stain (Thermo Scientific, Waltham, MA) for 1 h at room temperature. The plate was washed with PBS and imaged on the ImageXpress Micro system (Molecular Devices, San Jose, CA). Data quantification was performed in the same software suite as image acquisition.

2.8. Immunoprecipitation

PARP7 overexpression was induced with 1 $\mu\text{g}/\text{mL}$ doxycycline for 24 h in SK-MES-1 cells carrying the lentivirus-transduced transgene. Cell lysate was prepared as described above. PARP7 expression levels and differential MAR/PAR banding patterns were confirmed with a PARP7 antibody developed in-house and the MAR/PAR antibody by Western blot. One hundred μL Afi1521 macrodomain-coupled magnetic resin was pre-washed in PBS with 500 mM NaCl before adding to 500 μL lysate. ADP-ribosylated proteins were pulled down by incubation with the Afi1521 affinity resin for 1 h at 4 $^{\circ}\text{C}$. The resin was washed three times in PBS followed by elution in 100 μL 1X sample loading buffer at 65 $^{\circ}\text{C}$ for 5 min. The samples were then subjected to label-free quantitative mass spectrometry as described below.

For substrate hit validation, eluates from the Afi1521 pulldown were probed on Western blots for the relative abundance of overexpressed PARP7, as detected by the SBP antibody (1:1000 dilution), as well as DDX5, RBM14, hnRNP H1, and AHR with respective antibodies at manufacturer's recommended dilutions. Conversely, DDX5, RBM14, hnRNP H1, and AHR were immunoprecipitated to measure the relative ADP-ribosylation level with and without PARP7 overexpression. Immunoprecipitation was performed using DDX5, RBM14, hnRNP H1,

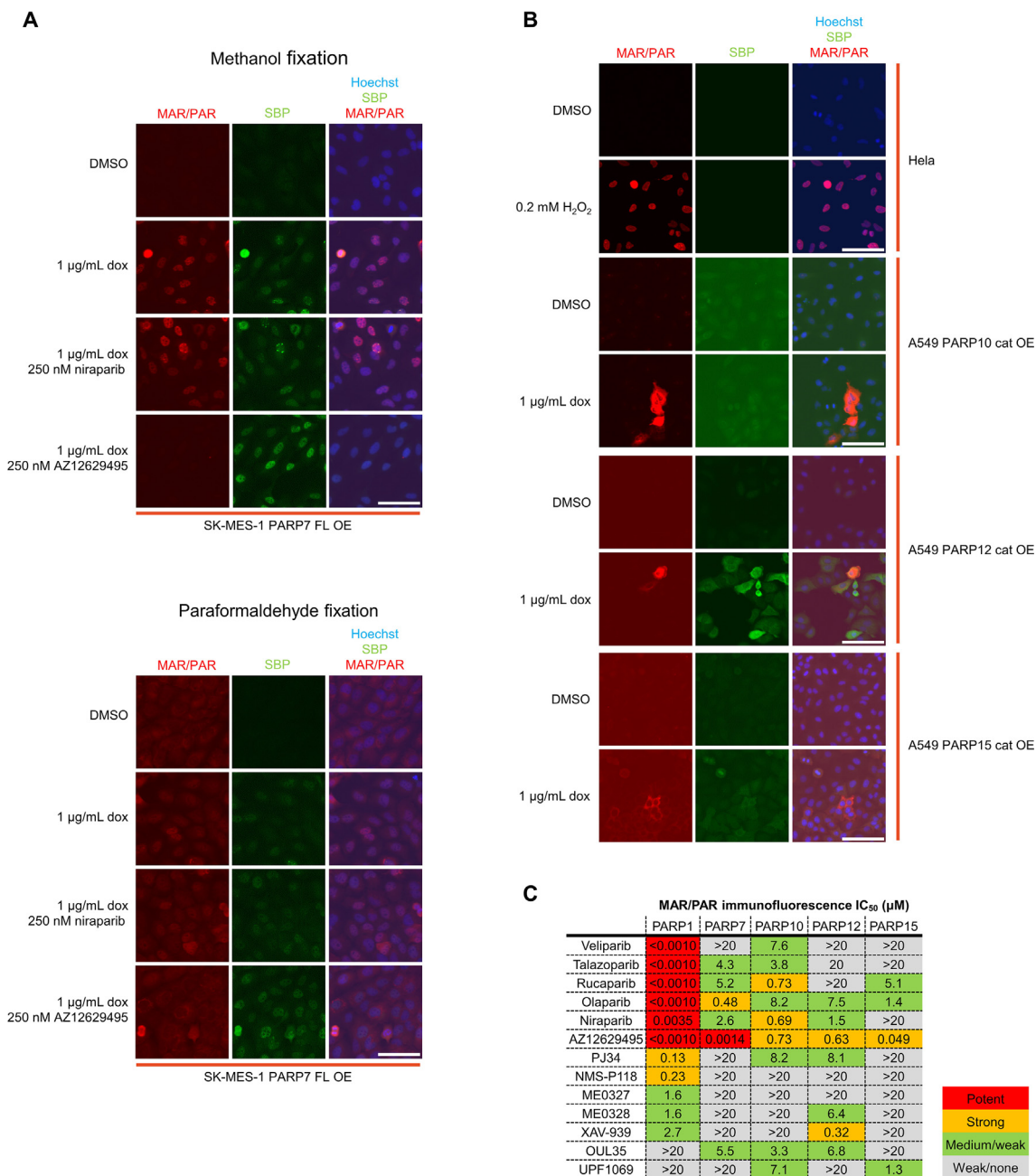


Fig. 3. MAR/PAR antibody is suitable for establishing cell biochemical assays of PARP activity. A) Comparison of immunofluorescence with MAR/PAR antibody and anti-SBP in SK-MES-1 cells stably overexpressing PARP7 after methanol (MeOH; top) or paraformaldehyde (PFA; bottom) fixation. Scale bars = 100 µm. B) Immunofluorescence staining of HeLa or A549 cells expressing various PARPs. Top two panels show staining of HeLa cells with or without PARP1 activation by hydrogen peroxide. PARP10, 12, and 15 assays show staining of A549 cells overexpressing the catalytic domain of these monoPARPs. Scale bars = 100 µm. C) PARP inhibitors were tested in duplicates in the various PARP assays using cell lines described in A) and B) based on MAR/PAR antibody immunofluorescence staining. Inhibition was ranked based on the following IC₅₀ cutoffs: potent, < 10 nM; strong, 10 nM–1 µM; medium/weak, 1 µM–10 µM; weak/none, > 10 µM.

or AHR antibodies coupled to Dynabeads Protein G resin (Thermo Fisher Scientific, Waltham, MA) according to the manufacturer’s recommended protocol. In this case, both the immunoprecipitation antibodies and the detection antibody (MAR/PAR from Cell Signaling Technologies) were raised in rabbit. To avoid detection of the immunoprecipitation antibodies with the goat anti-rabbit secondary antibody, the LI-COR QuickWestern reagent was used instead for secondary detection, which detected the folded MAR/PAR antibody on the Western blot but not the denatured antibodies use for immunoprecipitation.

2.9. Mass spectrometry data acquisition and analysis

Af1521 immunoprecipitation eluates were submitted to MS Bioworks (Ann Arbor, MI) for mass spectrometric sample preparation and analysis. Each sample was separated to ~1.5 cm on a 10% Bis-Tris Novex mini-gel (Thermo Fisher Scientific, Waltham, MA) in MES buffer system. The gel was stained with Coomassie Brilliant Blue (Thermo Fisher Scientific, Waltham, MA) and excised into ten equally-sized segments, which were processed using a ProGest – DigiLab robot (Accela, Prague, Czech Republic). They were washed with 25 mM ammonium bicarbonate followed by acetonitrile, reduced with 10 mM

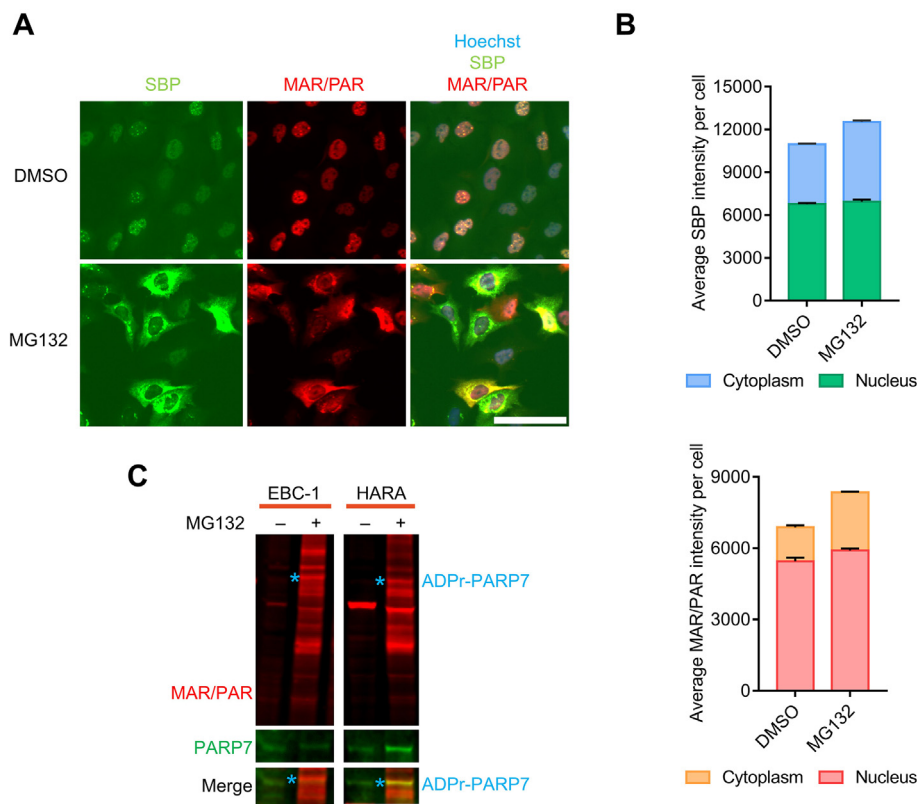


Fig. 4. Proteasome inhibition increases PARP7 and ADP-ribosylation levels. A) SK-MES-1 cells over-expressing SBP-tagged PARP7 were stained with anti-SBP and anti-MAR/PAR antibodies. Cells were treated with DMSO or 2 μ M MG132 for 16 h prior to methanol fixation and staining. Scale bar = 100 μ m. B) Quantification of the average MAR/PAR and SBP intensity in the cytoplasm and nucleus of cells treated as described in A. Error bars represent SD of three biological replicates. C) Western blots of whole cell lysates of EBC-1 and HARA with and without 2 μ M MG132 treatment for 16 h.

dithiothreitol at 60 °C followed by alkylation with 50 mM iodoacetamide at room temperature. Finally, the samples were digested with trypsin (Promega, Madison, WI) at 37 °C for 4 h, and quenched with formic acid. The gel digests were analyzed by nano-LC/MS/MS with a Waters (Milford, MA) NanoAcquity HPLC system coupled to a Thermo Fisher Q Exactive. Peptides were loaded on a trapping column and eluted over a 75 μ m analytical column at 350 nL/min. Both columns were packed with Luna C18 resin (Phenomenex, Torrance, CA). The mass spectrometer was operated in data-dependent mode, with MS and MS/MS performed in the Orbitrap at 70,000 FWHM resolution and 17,500 FWHM resolution, respectively. The fifteen most abundant ions were selected for MS/MS.

Mascot DAT files were parsed into the Scaffold software (Proteome Software, Portland, OR) for validation, filtering and to create a non-redundant list per sample. Data were filtered at 1% protein and peptide level false-discovery rate and requiring at least two unique peptide per protein.

2.10. Geneset enrichment analysis

Geneset enrichment analysis was performed on the list of putative PARP7 substrates. Putative substrates were defined as proteins with at least four spectral counts in total and a 1.5 fold-change increase or greater in spectral counts normalized by protein molecular weights due to doxycycline. The enrichment analysis was performed using hypergeometric tests for Gene Ontology and KEGG annotations with all the detected proteins as the background. The analysis was conducted with the statistical package “clusterProfiler” [43] within R, a free software environment for statistical computing and graphics (<http://www.R-project.org/>).

3. Results

3.1. Comparison of three commercially available ADP-ribose binding reagents

To characterize the three commercially available MAR binding reagents—the macrodomain-based pan-ADP-ribose and anti-mono-ADP-ribose binding reagents from EMD Millipore, and the MAR/PAR antibody from Cell Signaling Technology—a panel of modified recombinant proteins were generated. PARP1, PARP3, and cholera toxin A were auto-ADP-ribosylated by incubating them with NAD⁺, while histone H3 and BSA or Blue Carrier (BC) conjugated with a peptide were modified using PARP10 catalytic domain. These ADP-ribosylated proteins represented both PARYlation and MARYlation, as well as a diversity of modification sites by three different human PARPs and the bacterial cholera toxin A. The unmodified and modified proteins were tested on a dot blot format using the three affinity reagents (Fig. 1A). All three reagents demonstrated specific recognition of the ADP-ribosylated proteins while generating minimal signal from the unmodified proteins. To compare the relative reactivity, the protein spots were stained with the REVERT protein stain and used that to normalize the intensity from antibody binding. The anti-mono-ADP-ribose binding reagent, which is based on the PARP14 macrodomains, showed preferential binding to ADP-ribosylated PARP3 over ADP-ribosylated PARP1 relative to the Af1521-based anti-pan-ADP-ribose binding domain. The MAR/PAR antibody showed superior sensitivity in this assay compared to either of the other two binding reagents (Fig. 1B).

Next, these reagents were tested to see if they are able to detect ADP-ribosylated proteins directly from cell lysate. To generate samples with increased PARP activity, PARP16 was transiently overexpressed to induce auto-ADP-ribosylation of PARP16 in HeLa cells with the endogenous PARP16 knocked out via CRISPR/Cas9. As a control, these cells were transiently transfected with a plasmid carrying PARP16 catalytically dead mutant (H152Q, Y182A). Western blots were then performed with lysates from these cells (Fig. 1C-D) and showed that

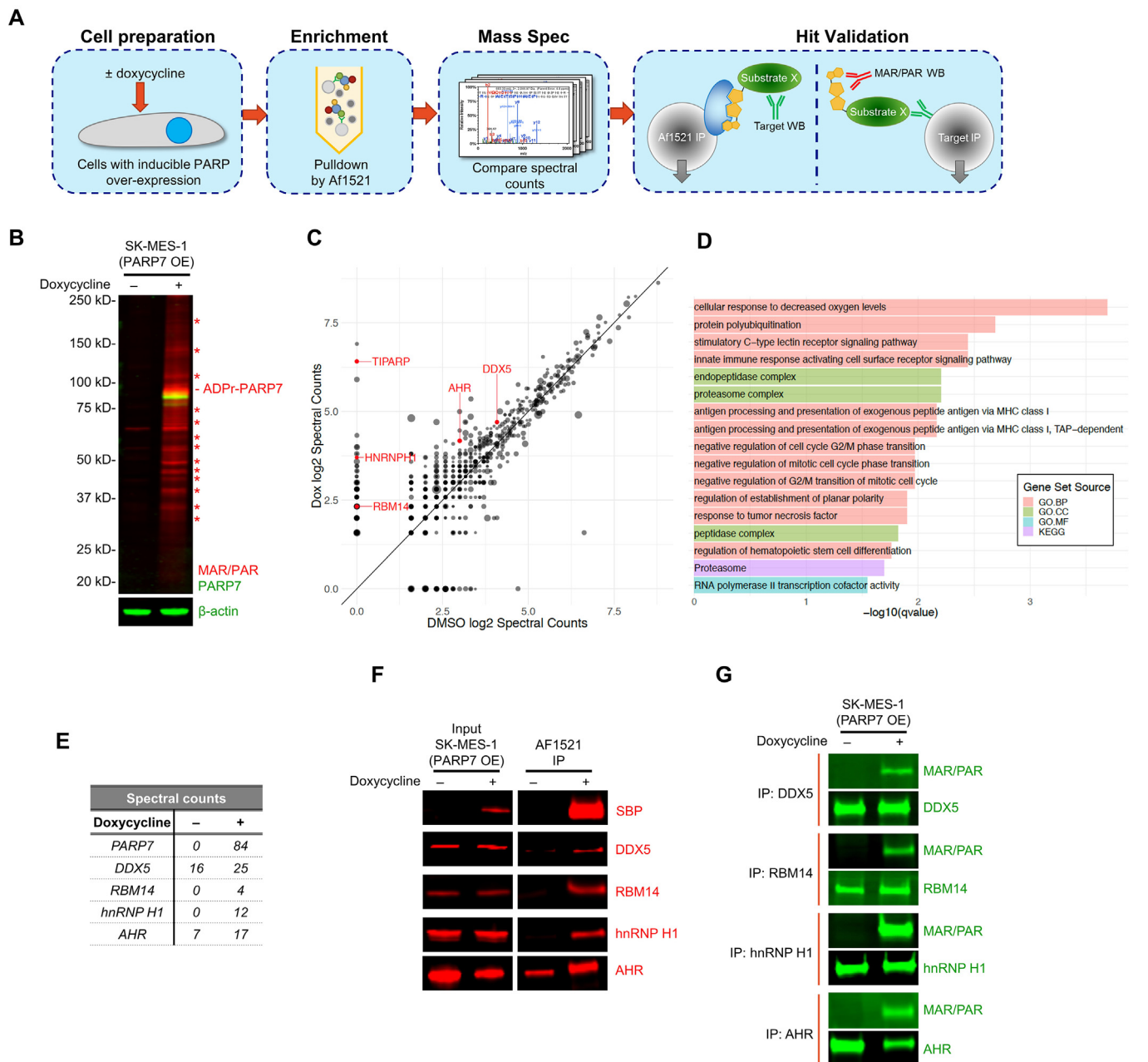


Fig. 5. PARP7 substrate identification and validation. A) Generalized workflow of substrate identification and validation. Cells are treated with doxycycline to induce exogenous expression of a particular PARP and thereby elevate ADP-ribosylation activity. ADP-ribosylated substrates are then enriched using Af1521-coupled resin. Whole eluates are processed and analyzed by label-free quantitative mass spectrometry to generate a list of putative hits, which are then validated by immunoprecipitation and Western blot analysis. B) Lysate samples of PARP7-overexpressing SK-MES-1 cells with or without doxycycline treatment showed differential MAR/PAR banding patterns. Putative PARP7 substrates are denoted by red asterisks. C) Log-transformed spectral counts (SpC) of all detected proteins from Af1521 pulldown in DMSO- or doxycycline-treated cells. Point size corresponds to protein molecular weight. Five validated PARP7 substrate proteins are highlighted in red. D) Significance levels of the top Gene Ontology and KEGG annotation gene enrichment analysis results for putative PARP7 substrates tested against all detected proteins as background. The putative protein set was selected based on fold-change ≥ 1.5 and total SpC ≥ 4 . A simplified representative set of Biological Process results are shown, removing nodes with levels higher than six and collapsing similar annotation nodes. E) SpC of PARP7, DDX5, RBM14, hnRNP H1, and AHR. F) Af1521 affinity purification led to greatly enriched PARP7, DDX5, RBM14, hnRNP H1, and AHR in SK-MES-1 from lysates following doxycycline-mediated induction of PARP7 overexpression versus lysates from non-induced cells. G) MAR/PAR antibody specifically detected ADP-ribosylation of DDX5, RBM14, hnRNP H1, and AHR in immunoprecipitated lysates from PARP7-overexpressing SK-MES-1 cells after doxycycline induction.

transfection, independent of PARP16 catalytic activity, induced PARylation as confirmed by the PAR-binding 10H antibody. The anti-pan-ADP-ribose binding reagent also produced similar banding pattern indicative of PARylation, whereas the anti-mono-ADP-ribose binding reagent did not. Importantly, only the MAR/PAR antibody was sensitive enough in this assay to detect auto-ADP-ribosylated PARP16, consistent with the results from the dot blot assay; no such signal was apparent in

lysates prepared from the catalytically-dead PARP16 lysate. Accordingly, focus was placed on further applying the MAR/PAR antibody in other types of assays.

3.2. Characterization of the MAR/PAR antibody binding epitope

Generally, elevated PAR background is observed after transient

transfection. Therefore, a cell line was generated to stably overexpress PARP7 under the control of a doxycycline-inducible promoter, and this was used to further characterize the MAR/PAR antibody. Western blots performed with the MAR/PAR antibody demonstrated that induction of PARP7 overexpression produced strong MAR/PAR banding patterns (Fig. 1E). The MAR/PAR antibody was also incubated with a variety of blocking molecules to deduce the binding epitope of this antibody. Blocking with ADP-ribose, NAD⁺, ATP, AMP and FAD all completely eliminated the banding pattern normally seen with the MAR/PAR antibody, which suggests that AMP is the minimal epitope. Adenosine also reduced antibody binding—but not thymidine, cytidine, or guanosine—confirming that this antibody at least in part recognizes the adenosine moiety and requires the phosphate group for binding (Fig. 1E).

3.3. Overexpression of PARPs leads to ADP-ribosylation banding patterns

Using the MAR/PAR antibody, overexpression of other PARPs was tested whether it would also produce similar ADP-ribosylation banding patterns. To achieve this, additional stable cell lines were generated with doxycycline-inducible overexpression of PARP10, PARP12, or PARP15. Western blot analysis of lysates from these cells indicated that overexpressing either the catalytic domain mutant or full length PARP produced ADP-ribosylation banding patterns (Fig. 2A–B). In A549, both PARP10 and PARP12 overexpression led to auto-modification, which generally shifted their molecular weights higher compared to the unmodified proteins. Additional ADP-ribosylation bands for cells overexpressing PARP7, PARP12, and PARP15 were observed which might be their cellular substrates.

Interestingly, ADP-ribosylation patterns in the engineered HeLa cell lines were weaker compared to the A549 lines, even though the relative expression levels were similar (Fig. 2A). This indicates that PARP activity is dependent on the cellular context, with factors such as substrate abundance, hydrolase activity, or cellular pathways influencing how PARPs function in different cellular settings. With this type of engineered system, one could begin answering fundamental questions about specific PARP substrates, how different PARPs are activated and modulated, and what are the differential roles of PARPs in different cell types.

3.4. Immunofluorescence staining and compound screening with the MAR/PAR antibody

Based on the robust signal observed by Western blotting, the MAR/PAR antibody was tested whether it is suitable for staining cells, with the goal of establishing a high-throughput assay for rapid compound screening. Methanol fixation was determined to be compatible with the use of this antibody for immunofluorescence staining, whereas paraformaldehyde fixation was not (Fig. 3A). Using methanol-fixed SK-MES-1 cells that inducibly overexpress PARP7, the MAR/PAR antibody was shown to be capable of detecting ADP-ribosylation as a result of PARP7 overexpression, which was simultaneously measured by staining of the N-terminal SBP-tag on PARP7. The strength of the ADP-ribosylation signal in this assay was greatly reduced by treatment with AZ12629495 (patent WO 2016/116602) reported to inhibit PARP7 activity but not by the PARP1-selective inhibitor niraparib, confirming that this assay is specifically reporting PARP7 MARYlation activity. A similar assay was performed to measure PARP1 activity, in which hydrogen peroxide is used to induce PARYlation in wild-type HeLa cells (Fig. 3B), and again showed that this antibody detected a specific signal. Finally, the MAR/PAR antibody was demonstrated to consistently generate a specific and quantifiable signal upon doxycycline-induction in A549 cell lines overexpressing the catalytic domains of PARP10, PARP12, or PARP15 (Fig. 3B).

Having demonstrated the selective detection of PARP activity with this antibody, a screen was performed on a variety of previously developed PARP inhibitors in the same assays (Fig. 3C). Known PARP1

inhibitors such as veliparib, talazoparib, rucaparib, olaparib, and niraparib were shown to strongly inhibit PARP1-mediated ADP-ribosylation in the assay, while generally exerting weaker or no inhibition on the monoPARPs (PARP7, PARP10, PARP12 and PARP15) that were tested. AZ12629495 showed a range of inhibitory activities against all five of the PARPs tested, ranging from a sub-nanomolar IC₅₀ for PARP1 to a sub-micromolar IC₅₀ for PARP10 (Fig. 3C). To our knowledge, this represents the first cellular high-throughput MARYlation assay to be reported in the literature.

3.5. Proteasome inhibition in PARP7 overexpressing cells

Next, this assay system was tested to assess whether ADP-ribosylation could be used as readout to evaluate modulators of PARP activity. It has been reported in the literature that proteasome inhibition leads to increased levels of PARP7 [44,45]. Treatment of the PARP7-overexpressing SK-MES-1 cells with the proteasome inhibitor MG132 resulted in cytoplasmic accumulation of PARP7 and increased ADP-ribosylation level as determined by immunofluorescence staining with the SBP and MAR/PAR antibody, respectively (Fig. 4A–B). A higher average MAR/PAR intensity per cell in the cytosol was observed after MG132 treatment, suggesting that proteasome-mediated degradation may play a role in modulating the levels of PARP7 and substrate proteins (Fig. 4B). Immunofluorescence was used to assess the impact of proteasome inhibition on the EBC-1 and HARA squamous lung cell carcinoma lines, which express endogenous levels of PARP7 (Fig. 4C). The Western blot showed a marked increase in PARP7 expression in both cell lines upon MG132 treatment, as well as the appearance of extensive ADP-ribosylation banding patterns. These observations support the reported hypothesis that PARP7 mediates degradation of its substrate proteins, such as the aryl hydrogen receptor (AHR), through the proteasome system [46]. More importantly, these experiments validate the utility of the MAR/PAR antibody to evaluate the cellular ADP-ribosylation status upon stimulation, which is critical to link PARP activity to their function.

3.6. Identification and validation of PARP7 substrates using ADP-ribose binding reagents

To identify PARP substrates, a generalizable workflow using commercially available binding reagents and standard mass spectrometry methods has been established (Fig. 5A). Using PARP7 as a test case, lysates from SK-MES-1 cells were generated in the presence or absence of doxycycline to induce PARP7 overexpression (Fig. 5B). The ADP-ribosylated proteins were immunoprecipitated with the macrodomain Af1521-coupled magnetic resin. The eluates were analyzed by label-free quantitative mass spectrometry to compare the relative abundance of the isolated proteins and thereby generate a list of putative PARP7 substrates.

The mass spectrometric analysis identified a total of 954 proteins, with 202 of those showing an increase in spectral counts of at least 1.5 fold following induction of PARP7 overexpression and a total spectral count of at least 4 (Fig. 5C). ADP-ribosylated PARP7 was enriched as shown by Af1521 immunoprecipitation followed by detection with the SBP antibody, and this was used to validate immunoprecipitated samples before subjecting them to mass spectrometry (Fig. 5F). Based on these hits, a gene set enrichment analysis was performed against all identified proteins as background (Fig. 5D). Interestingly, gene ontology terms such as “proteasome complex” and “protein polyubiquitination” returned as enriched gene sets, supporting that PARP7 may be linked to the proteasome system. Several hits were selected for validation by immunoprecipitation and Western blotting, including DEAD-box helicase 5 (DDX5), RNA-binding protein 14 (RBM14), Heterogeneous nuclear ribonucleoprotein H (hnRNP H1), and aryl hydrocarbon receptor (AHR) (Fig. 5E). Considerable enrichment of DDX5, RBM14, hnRNP H1, and AHR was observed following Af1521 affinity-

purification from cells that had undergone doxycycline induction relative to lysates from non-induced cells, providing further evidence that these proteins are substrates for PARP7 (Fig. 5F). To further confirm this, the reverse experiment was performed, in which the target proteins were immunoprecipitated with the appropriate antibodies and then probed for ADP-ribosylation using the MAR/PAR antibody (Fig. 5G). These results mirrored the findings in the previous immunoprecipitation experiment, with clear ADP-ribosylation signal observed on all of these proteins from cell lysates with elevated PARP7 activity due to overexpression.

4. Discussion

A cell-based biochemical assay platform to study PARP biology is reported here, as well as a generalizable workflow to identify PARP substrates. These assays will enable the identification and characterization of compounds that directly modulate PARP activity in cells. In parallel, the substrate identification approach presented here will help expand the knowledge of PARP biology by making it possible to link cellular pathways to the enzymatic activities of specific PARPs. These exploratory experiments offer a starting point for more in-depth biochemical studies to understand the role of ADP-ribosylation in cellular processes and disease phenotypes.

The MAR/PAR antibody is a high-affinity tool that provides leverage for researchers in the field to study MARYlation. This antibody has proven useful for the development of multiple MARYlation assays, although it lacks the desired selectivity to discriminate MARYlation from PARYlation. Stable PARP overexpression cell lines were generated to avoid the increase in PARYlation generally observed with transient transfection. In the future, the PARP community would benefit from access to a high-affinity MAR-selective antibody, which would eliminate the PAR background signal that otherwise masks the weaker MAR signal. When such reagents become available, the assays reported in this study could be adapted by swapping out the MAR/PAR antibody in order to assess the performance of any MAR-specific antibodies.

Very low basal MARYlation is generally observed *in vitro*, as detected by existing ADP-ribose detection reagents. In this study, several ways were explored to increase monoPARP activity by overexpressing the PARPs of interest or by using the proteasome inhibitor, MG132. Multiple mechanisms have been proposed that control ADP-ribosylation levels in the cell. ADP-ribosylation of AHR by PARP7 is thought to target AHR for proteasome degradation, and this effect is countered by the hydrolase activity of MacroD1 [29,46,47]. Cellular stress signals also appear to be an important mechanism for stimulating monoPARP activity. PARP12 has been reported as an interferon-stimulated gene that is critical for antiviral response after Zika virus infection [48]. Similarly, PARP14 has been shown to be induced by inflammatory stimuli and to modulate subcellular localization of type I interferon-inducible proteins [49]. The assays presented here may therefore prove helpful in understanding the role of MARYlation in response to inflammatory signaling or other stress conditions. For instance, the immunofluorescence assay could be used to rapidly screen pathway agonists and growth conditions to evaluate their effects in a particular cell line or on the activity of a particular PARP. These experiments can be complemented by substrate identification and gene set enrichment analysis to deduce the role of PARPs in a particular pathway.

MonoPARPs make up the majority of the PARP family and mediate important biological functions [6,50], and their roles in various stress response mechanisms, such as unfolded protein response [25], NF- κ B signaling [51], antiviral response [52,53], and cytokine signaling [54,55], potentially make them attractive targets in many diseases. To develop monoPARPs as future therapeutic targets, it will be important to establish relevant biomarkers of PARP activity. The identification and validation of monoPARP substrates would make it possible to measure PARP activity *in vivo*, and such assays would be ideal as they offer a direct report of enzymatic activity. However, measuring

substrate ADP-ribosylation at specific peptide sequences remains challenging due to the lack of site-specific antibodies. The development of such antibodies may now be possible, as methods for binding site identification and ADP-ribose peptide synthesis have improved over the past few years [56–61]. In the meantime, other surrogate assays for reporting on downstream activity of affected pathways are currently being used to measure the pharmacodynamics of monoPARP inhibitors. For example, Chk1 phosphorylation at S345 has been used to measure PARP6 inhibition in HCC1806 cell line-derived tumors [23]. In the future, direct measurement of ADP-ribosylation of substrate proteins would offer better assessment of drug action and help to identify drugs that exhibit pleiotropic and off-target effects as a consequence of having less favorable selectivity profiles.

Declaration of Competing Interest

The authors who have taken part in this study are employees of Ribon Therapeutics, Inc., which fully funded this study, and declare no conflict of interest with respect to this manuscript.

Acknowledgements

The authors thank all current and past members of Ribon Therapeutics, Inc. for their work to enabling drug discovery for the PARP protein family. The authors thank Cell Signaling Technology for providing pre-commercial access to the MAR/PAR antibodies for evaluation and characterization, specifically Rami Najjar and Matthew Stokes for the collaboration and discussion. The authors thank Paul Chang for overseeing the initial generation of the SK-MES-1 PARP7 overexpressing cell line. The authors thank Michael Eisenstein for editing the manuscript.

References

- [1] A.K.L. Leung, PARPs, *Curr. Biol.* 27 (23) (2017) R1256–R1258.
- [2] M.O. Hottiger, P.O. Hassa, B. Luscher, H. Schuler, F. Koch-Nolte, Toward a unified nomenclature for mammalian ADP-ribosyltransferases, *Trends Biochem. Sci.* 35 (4) (2010) 208–219.
- [3] B.A. Gibson, W.L. Kraus, New insights into the molecular and cellular functions of poly(ADP-ribose) and PARPs, *Nat. Rev. Mol. Cell Biol.* 13 (7) (2012) 411–424.
- [4] A. Burkle, L. Virag, Poly(ADP-ribose): PARadigms and PARadoxes, *Mol. Aspects Med.* 34 (6) (2013) 1046–1065.
- [5] C.A. Viveiro, A.K. Leung, Proteomics approaches to identify mono-(ADP-ribosyl)ated and poly(ADP-ribosyl)ated proteins, *Proteomics* 15 (2–3) (2015) 203–217.
- [6] R. Gupte, Z. Liu, W.L. Kraus, PARPs and ADP-ribosylation: recent advances linking molecular functions to biological outcomes, *Genes Dev.* 31 (2) (2017) 101–126.
- [7] P. Bai, Biology of poly(ADP-Ribose) polymerases: the factotums of cell maintenance, *Mol. Cell.* 58 (6) (2015) 947–958.
- [8] H. Kawamitsu, H. Hoshino, H. Okada, M. Miwa, H. Momoi, T. Sugimura, Monoclonal antibodies to poly(adenosine diphosphate ribose) recognize different structures, *Biochemistry* 23 (16) (1984) 3771–3777.
- [9] J. Fahrner, R. Kranaster, M. Altmeyer, A. Marx, A. Burkle, Quantitative analysis of the binding affinity of poly(ADP-ribose) to specific binding proteins as a function of chain length, *Nucleic Acids Res.* 35 (21) (2007) e143.
- [10] J.P. Gagne, M. Isabelle, K.S. Lo, S. Bourassa, M.J. Hendzel, V.L. Dawson, et al., Proteome-wide identification of poly(ADP-ribose) binding proteins and poly(ADP-ribose)-associated protein complexes, *Nucleic Acids Res.* 36 (22) (2008) 6959–6976.
- [11] J.P. Gagne, E. Pic, M. Isabelle, J. Krietsch, C. Ethier, E. Paquet, et al., Quantitative proteomics profiling of the poly(ADP-ribose)-related response to genotoxic stress, *Nucleic Acids Res.* 40 (16) (2012) 7788–7805.
- [12] M. Isabelle, J.P. Gagne, I.E. Gallouzi, G.G. Poirier, Quantitative proteomics and dynamic imaging reveal that G3BP-mediated stress granule assembly is poly(ADP-ribose)-dependent following exposure to MNGG-induced DNA alkylation, *J. Cell. Sci.* 125 (Pt 19) (2012) 4555–4566.
- [13] N. Dani, A. Stilla, A. Marchegiani, A. Tamburro, S. Till, A.G. Ladurner, et al., Combining affinity purification by ADP-ribose-binding macro domains with mass spectrometry to define the mammalian ADP-ribosyl proteome, *Proc. Natl. Acad. Sci. USA* 106 (11) (2009) 4243–4248.
- [14] S. Jungmichel, F. Rosenthal, M. Altmeyer, J. Lukas, M.O. Hottiger, M.L. Nielsen, Proteome-wide identification of poly(ADP-Ribosyl)ation targets in different genotoxic stress responses, *Mol. Cell.* 52 (2) (2013) 272–285.
- [15] B.A. Gibson, L.B. Conrad, D. Huang, W.L. Kraus, Generation and characterization of recombinant antibody-like ADP-ribose binding proteins, *Biochemistry* 56 (48) (2017) 6305–6316.

- [16] R. Bredehorst, K. Wielckens, P. Adamietz, E. Steinhagen-Thiessen, H. Hilz, Mono (ADP-ribosyl)ation and poly(ADP-ribosyl)ation of proteins in developing liver and in hepatomas: relation of conjugate subfractions to metabolic competence and proliferation rates, *Eur. J. Biochem.* 120 (2) (1981) 267–274.
- [17] K. Wielckens, R. Bredehorst, P. Adamietz, H. Hilz, Protein-bound polymeric and monomeric ADP-ribose residues in hepatic tissues. Comparative analyses using a new procedure for the quantification of poly(ADP-ribose), *Eur. J. Biochem.* 117 (1) (1981) 69–74.
- [18] Y. Zhang, J. Wang, M. Ding, Y. Yu, Site-specific characterization of the Asp- and Glu-ADP-ribosylated proteome, *Nat. Methods* 10 (10) (2013) 981–984.
- [19] K. Islam, The bump-and-hole tactic: expanding the scope of chemical genetics, *Cell Chem. Biol.* 25 (10) (2018) 1171–1184.
- [20] I. Carter-O'Connell, H. Jin, R.K. Morgan, L.L. David, M.S. Cohen, Engineering the substrate specificity of ADP-ribosyltransferases for identifying direct protein targets, *J. Am. Chem. Soc.* 136 (14) (2014) 5201–5204.
- [21] B.A. Gibson, Y. Zhang, H. Jiang, K.M. Hussey, J.H. Shrimp, H. Lin, et al., Chemical genetic discovery of PARP targets reveals a role for PARP-1 in transcription elongation, *Science* 353 (6294) (2016) 45–50.
- [22] I. Carter-O'Connell, A. Vermehren-Schmaedick, H. Jin, R.K. Morgan, L.L. David, M.S. Cohen, Combining chemical genetics with proximity-dependent labeling reveals cellular targets of poly(ADP-ribose) polymerase 14 (PARP14), *ACS Chem. Biol.* 13 (10) (2018) 2841–2848.
- [23] Z. Wang, S.E. Grosskurth, T. Cheung, P. Pletteri, J. Zhang, X. Wang, et al., Pharmacological inhibition of PARP6 triggers multipolar spindle formation and elicits therapeutic effects in breast cancer, *Cancer Res.* (2018).
- [24] I.T. Kirby, A. Kojic, M.R. Arnold, A.G. Thorsell, T. Karlberg, A. Vermehren-Schmaedick, et al., Potent and selective PARP11 inhibitor suggests coupling between cellular localization and catalytic activity, *Cell Chem. Biol.* (2018).
- [25] M. Jwa, P. Chang, PARP16 is a tail-anchored endoplasmic reticulum protein required for the PERK- and IRE1 α -mediated unfolded protein response, *Nat. Cell Biol.* 14 (11) (2012) 1223–1230.
- [26] Y. Zhao, X. Hu, L. Wei, D. Song, J. Wang, L. You, et al., PARP10 suppresses tumor metastasis through regulation of Aurora A activity, *Oncogene* 37 (22) (2018) 2921–2935.
- [27] E.M. Schleicher, A.M. Galvan, Y. Imamura-Kawawasa, G.L. Moldovan, C.M. Nicolae, PARP10 promotes cellular proliferation and tumorigenesis by alleviating replication stress, *Nucleic Acids Res.* 46 (17) (2018) 8908–8916.
- [28] L. MacPherson, L. Tamblin, S. Rajendra, F. Bralha, J.P. McPherson, J. Matthews, 2,3,7,8-Tetrachlorodibenzo-p-dioxin poly(ADP-ribose) polymerase (TiPARP, ARTD14) is a mono-ADP-ribosyltransferase and repressor of aryl hydrocarbon receptor transactivation, *Nucleic Acids Res.* 41 (3) (2013) 1604–1621.
- [29] A. Gomez, C. Bindsboll, V.S. Somisetty, G. Grimaldi, D. Hutin, L. MacPherson, et al., Characterization of TCDD-inducible poly-ADP-ribose polymerase (TiPARP/ARTD14) catalytic activity, *Biochem. J.* (2018).
- [30] B. Kaufman, R. Shapira-Frommer, R.K. Schmutzler, M.W. Audeh, M. Friedlander, J. Balmana, et al., Olaparib monotherapy in patients with advanced cancer and a germline BRCA1/2 mutation, *J. Clin. Oncol.* 33 (3) (2015) 244–250.
- [31] G. Kim, G. Ison, A.E. McKee, H. Zhang, S. Tang, T. Gwise, et al., FDA approval summary: olaparib monotherapy in patients with deleterious germline BRCA-mutated advanced ovarian cancer treated with three or more lines of chemotherapy, *Clin. Cancer Res.* 21 (19) (2015) 4257–4261.
- [32] F.G. Soriano, L. Virag, C. Szabo, Diabetic endothelial dysfunction: role of reactive oxygen and nitrogen species production and poly(ADP-ribose) polymerase activation, *J. Mol. Med. (Berl.)* 79 (8) (2001) 437–448.
- [33] Y. Shen, F.L. Rehman, Y. Feng, J. Boshuizen, I. Bajrami, R. Elliott, et al., BMN 673, a novel and highly potent PARP1/2 inhibitor for the treatment of human cancers with DNA repair deficiency, *Clin. Cancer Res.* 19 (18) (2013) 5003–5015.
- [34] C.K. Donawho, Y. Luo, Y. Luo, T.D. Penning, J.L. Bauch, J.J. Bouska, et al., ABT-888, an orally active poly(ADP-ribose) polymerase inhibitor that potentiates DNA-damaging agents in preclinical tumor models, *Clin. Cancer Res.* 13 (9) (2007) 2728–2737.
- [35] A.E. Lindgren, T. Karlberg, A.G. Thorsell, M. Hesse, S. Spjut, T. Ekblad, et al., PARP inhibitor with selectivity toward ADP-ribosyltransferase ARTD3/PARP3, *ACS Chem. Biol.* 8 (8) (2013) 1698–1703.
- [36] H. Sharif-Askari, L. Amrein, R. Aloyz, L. Panasci, PARP3 inhibitors ME0328 and olaparib potentiate vinorelbine sensitization in breast cancer cell lines, *Breast Cancer Res. Treat.* 172 (1) (2018) 23–32.
- [37] S.M. Huang, Y.M. Mishina, S. Liu, A. Cheung, F. Stegmeier, G.A. Michaud, et al., Tankyrase inhibition stabilizes axin and antagonizes Wnt signalling, *Nature* 461 (7264) (2009) 614–620.
- [38] H. Venkannagari, P. Verheugd, J. Koivunen, T. Haikarainen, E. Obaji, Y. Ashok, et al., Small-molecule chemical probe rescues cells from mono-ADP-ribosyltransferase ARTD10/PARP10-induced apoptosis and sensitizes cancer cells to DNA damage, *Cell Chem. Biol.* 23 (10) (2016) 1251–1260.
- [39] R. Kristeleit, G.I. Shapiro, H.A. Burris, A.M. Oza, P. LoRusso, M.R. Patel, et al., A Phase I-II study of the oral PARP inhibitor rucaparib in patients with germline BRCA1/2-mutated ovarian carcinoma or other solid tumors, *Clin. Cancer Res.* 23 (15) (2017) 4095–4106.
- [40] M.R. Mirza, B.J. Monk, J. Herrstedt, A.M. Oza, S. Mahner, A. Redondo, et al., Niraparib maintenance therapy in platinum-sensitive, recurrent ovarian cancer, *N. Engl. J. Med.* 375 (22) (2016) 2154–2164.
- [41] G. Papeo, H. Posteri, D. Borghi, A.A. Busel, F. Caprera, E. Casale, et al., Discovery of 2-[1-(4,4-difluorocyclohexyl)piperidin-4-yl]-6-fluoro-3-oxo-2,3-dihydro-1H-isoindole-4-carboxamide (NMS-P118): a potent, orally available, and highly selective PARP-1 inhibitor for cancer therapy, *J. Med. Chem.* 58 (17) (2015) 6875–6898.
- [42] F. Moroni, L. Formentini, E. Gerace, E. Camaioni, D.E. Pellegrini-Giampietro, A. Chiarugi, et al., Selective PARP-2 inhibitors increase apoptosis in hippocampal slices but protect cortical cells in models of post-ischaemic brain damage, *Br. J. Pharmacol.* 157 (5) (2009) 854–862.
- [43] G. Yu, L.G. Wang, Y. Han, Q.Y. He, clusterProfiler: an R package for comparing biological themes among gene clusters, *OMICS* 16 (5) (2012) 284–287.
- [44] N.A. Davarinis, R.S. Pollenz, Aryl hydrocarbon receptor imported into the nucleus following ligand binding is rapidly degraded via the cytosolic proteasome following nuclear export, *J. Biol. Chem.* 274 (40) (1999) 28708–28715.
- [45] H. Jin, S. Hu, G. Li, C. Tu, J. Yuan, B. Qiang, Isolation and identification of cDNA fragments and full-length cDNA differentially expressed in human glioblastoma cell line BT-325 versus all-trans retinoic acid induction, *Chin. Med. Sci. J.* 15 (4) (2000) 195–200.
- [46] J. Matthews, AHR toxicity and signaling: role of TiPARP and ADP-ribosylation, *Curr. Opin. Toxicol.* 2017 (2) (Feb. 2017) 50–57.
- [47] Q. Ma, K.T. Baldwin, 2,3,7,8-tetrachlorodibenzo-p-dioxin-induced degradation of aryl hydrocarbon receptor (AhR) by the ubiquitin-proteasome pathway. Role of the transcription activation and DNA binding of AhR, *J. Biol. Chem.* 275 (12) (2000) 8432–8438.
- [48] L. Li, H. Zhao, P. Liu, C. Li, N. Quanquin, X. Ji, et al., PARP12 suppresses Zika virus infection through PARP-dependent degradation of NS1 and NS3 viral proteins, *Sci. Signal.* 11 (535) (2018).
- [49] G. Caprara, E. Prosperini, V. Piccolo, G. Sigismondo, A. Melacarne, A. Cuomo, et al., PARP14 controls the nuclear accumulation of a subset of type I IFN-inducible proteins, *J. Immunol.* 200 (7) (2018) 2439–2454.
- [50] S. Vyas, P. Chang, New PARP targets for cancer therapy, *Nat. Rev. Cancer* 14 (7) (2014) 502–509.
- [51] P. Verheugd, A.H. Forst, L. Milke, N. Herzog, K.L. Feijs, E. Kremmer, et al., Regulation of NF- κ B signalling by the mono-ADP-ribosyltransferase ARTD10, *Nat. Commun.* 4 (2013) 1683.
- [52] T. Yamada, H. Horimoto, T. Kameyama, S. Hayakawa, H. Yamato, M. Dazai, et al., Constitutive aryl hydrocarbon receptor signaling constrains type I interferon-mediated antiviral innate defense, *Nat. Immunol.* 17 (6) (2016) 687–694.
- [53] Y. Zhang, D. Mao, W.T. Roswit, X. Jin, A.C. Patel, D.A. Patel, et al., PARP-DTX3L ubiquitin ligase targets host histone H2B β and viral 3C protease to enhance interferon signaling and control viral infection, *Nat. Immunol.* 16 (12) (2015) 1215–1227.
- [54] H. Iwata, C. Goettsch, A. Sharma, P. Ricchiuto, W.W. Goh, A. Halu, et al., PARP9 and PARP14 cross-regulate macrophage activation via STAT1 ADP-ribosylation, *Nat. Commun.* 7 (2016) 12849.
- [55] S.H. Cho, A. Raybuck, M. Wei, J. Erickson, K.T. Nam, R.G. Cox, et al., B cell-intrinsic and -extrinsic regulation of antibody responses by PARP14, an intracellular (ADP-ribosyl)transferase, *J. Immunol.* 191 (6) (2013) 3169–3178.
- [56] C.M. Daniels, S.E. Ong, A.K.L. Leung, ADP-ribosylated peptide enrichment and site identification: the phosphodiesterase-based method, *Methods Mol. Biol.* 1608 (2017) 79–93.
- [57] E. Bartlett, J.J. Bonfiglio, E. Prokhorova, T. Colby, F. Zobel, I. Ahel, et al., Interplay of histone marks with serine ADP-ribosylation, *Cell Rep.* 24 (13) (2018) 3488–502 e5.
- [58] L. Palazzo, O. Leidecker, E. Prokhorova, H. Dauben, I. Matic, I. Ahel, Serine is the major residue for ADP-ribosylation upon DNA damage, *Elife* (2018) 7.
- [59] D.M. Leslie Pedrioli, M. Leutert, V. Bilan, K. Nowak, K. Gunasekera, E. Ferrari, et al., Comprehensive ADP-ribosylome analysis identifies tyrosine as an ADP-ribose acceptor site, *EMBO Rep.* 19 (8) (2018).
- [60] J. Voorneveld, J.G.M. Rack, I. Ahel, H.S. Overkleeft, G.A. van der Marel, D.V. Filippov, Synthetic alpha- and beta-Ser-ADP-ribosylated peptides reveal alpha-Ser-ADPr as the native epimer, *Org. Lett.* 20 (13) (2018) 4140–4143.
- [61] Q. Liu, H.A.V. Kistemaker, S. Bhogaraju, I. Dikic, H.S. Overkleeft, G.A. van der Marel, et al., A general approach towards triazole-linked adenosine diphosphate ribosylated peptides and proteins, *Angew Chem. Int. Ed. Engl.* 57 (6) (2018) 1659–1662.